Dark Hanle resonances from selected segments of the Gaussian laser beam cross-section

A. J. Krmpot[1], S. M. Ćuk[1], S. N. Nikolić[1], M. Radonjić[1], D. G. Slavov[2], and B. M. Jelenković[1]

[1]Institute of Physics, University of Belgrade, Pregrevica 118, 11080 Belgrade, Serbia
[2]Institute of Electronics, Bulgarian Academy of Sciences, 72 Tzarigradsko Chaussee blvd., 1784 Sofia, Bulgaria
*krmpot@phy.bg.ac.rs

Abstract: We present the Hanle EIT resonances obtained from the various segments of the Gaussian laser beam cross-section, selected by moving the small aperture (placed in front of the detector) radially along the laser beam. Significant differences in the Hanle lineshapes are observed depending on whether the central or outer parts of the Gaussian laser beam are detected. The line narrowing and two counter-sign peaks occur at outer, less intense parts of the beam. The theoretical model suggests that the EIT lineshapes in the laser wings are result of the interference of the laser light and coherently prepared atoms coming from the central part of the beam. By blocking the central part of the laser beam in front of the detector, narrower, and for high laser intensities, even more contrasted Hanle resonances are obtained.

©2009 Optical Society of America

OCIS codes: (020.1670) Coherent optical effects; (270.1670) Coherent optical effects.

References and links

1. E. Arimondo, "Coherent population trapping in laser spectroscopy," Prog. Opt. **35**, 257–354 (1996).
2. G. Alzetta, A. Gozzini, L. Moi, and G. Orriolis, "An experimental method for the observation of RF transitions and laser beat resonances in oriented Na vapour," Nuovo Cim. **36**(1), 5–20 (1976).
3. S. E. Harris, J. E. Field, and A. Imamoglu, "Nonlinear Optical Processes Using Electromagnetically Induced Transparency," Phys. Rev. Lett. **64**(10), 1107–1110 (1990).
4. A. M. Akulshin, S. Barreiro, and A. Lezama, "Electromagnetically induced absorption and transparency due to resonant two-field excitation of quasidegenerate levels in Rb vapor," Phys. Rev. A **57**(4), 2996–3002 (1998).
5. G. Moruzzi and F. Strumia, "The Hanle effect and level crossing spectroscopy," (Plenum Press 1991).
6. C. Andreeva, S. Cartaleva, Y. Dancheva, V. Biancalana, A. Burchianti, C. Marinelli, E. Mariotti, L. Moi, and K. Nasyrov, "Coherent spectroscopy of degenerate two-level systems in Cs," Phys. Rev. A **66**(1), 502 (2002).
7. A. Javan, O. Kocharovskaya, H. Lee, and M. O. Scully, "Narrowing of electromagnetically induced transparency resonance in a Doppler-broadened medium," Phys. Rev. A **66**(1), 013805 (2002).
8. C. Y. Ye, and A. S. Zibrov, "Width of the electromagnetically induced transparency resonance in atomic vapor," Phys. Rev. A **65**(2), 023806 (2002).
9. A. J. Krmpot, M. M. Mijailović, B. M. Panić, D. V. Lukić, A. G. Kovacević, D. V. Pantelić, and B. M. Jelenković, "Sub-Doppler absorption narrowing in atomic vapor at two intense laser fields," Opt. Express **13**(5), 1448–1456 (2005).
10. F. Levi, A. Godone, J. Vanier, S. Micalizio, and G. Modugno, "Lineshape of dark line and maser emission profile in CPT," Eur. Phys. J. D **12**(1), 53–59 (2000).
11. A. V. Taichenachev, A. M. Tumaikin, V. I. Yudin, M. Stahler, R. Wynands, J. Kitching, and L. Hollberg, "Nonliear-resonance line shapes: Dependence on the transverse intensity distribution of a light beam," Phys. Rev. A **69**(2), 024501 (2004).
12. M. Radonjić, D. Arsenović, Z. Grujić, and B. M. Jelenković, "Coherent population trapping linewidths for open transitions: Cases of different transverse laser intensity distribution," Phys. Rev. A **79**(2), 023805 (2009).
13. H. Gilles, B. Cheron, O. Emile, F. Bretenaker, and A. Le Floch, "Rabi-Lorentzian profile of an Atomic Resonance Obtained with Gaussian Beams," Phys. Rev. Lett. **86**(7), 1175–1178 (2001).
14. I. Novikova, Y. Xiao, D. F. Phillips, and R. L. Walsworth, "EIT and diffusion of atomic coherence," J. Mod. Opt. **52**(16), 2381–2390 (2005).
15. Y. Xiao, I. Novikova, D. F. Phillips, and R. L. Walsworth, "Diffusion-Induced Ramsey Narrowing," Phys. Rev. Lett. **96**(4), 043601 (2006).
16. S. I. Kanorsky, A. Weis, and J. Skalla, "A wall-collision-induced Ramsey resonance," Appl. Phys. B **60**, S165 (1995).
17. C. Affolderbach, C. Andreeva, S. Cartaleva, T. Karaulanov, G. Mileti, and D. Slavov, "Light shift suppression in laser optically pumped vapour-cell atomic frequency standards," Appl. Phys. B **80**(7), 841–848 (2005).

18. J. Belfi, G. Bevilacqua, V. Biancalana, S. Cartaleva, Y. Dancheva, and L. Moi, "Cesium coherent population trapping magnetometer for cardiosignal detection in an unshielded environment," J. Opt. Soc. B **24**(9), 2357 (2007).
19. G. Wasik, W. Gawlik, J. Zachorowski, and W. Zawadzki, "Laser frequency stabilization by Doppler-free magnetic dichroism," Appl. Phys. B **75**(6-7), 613–619 (2002).
20. Z. D. Grujić, M. Mijailović, D. Arsenović, A. Kovačević, M. Nikolić, and B. M. Jelenković, "Dark Raman resonances due to Ramsey interference in vacuum vapor cells," Phys. Rev. A **78**(6), 063816 (2008).

1. Introduction

Coherent effects in Doppler broadened alkali atom vapor have been intensively investigated over the past decade. Coherent population trapping (CPT) [1, 2], electromagnetically induced transparency (EIT) [3], and electromagnetically induced absorption (EIA) [4] have been observed and examined in either pump-probe and in Hanle configuration [5, 6]. All these phenomena strongly depend on the intensity of the applied laser field. The dependence of CPT and EIT lineshapes on the laser intensity has been extensively studied [7–9].

Typical radial laser beam profile in experiments studying CPT and EIT is Gaussian. The intensities in the center and in the wings of the Gaussian beam are very different. Nevertheless, the order of magnitude lower intensity in the wings can still contribute to the atomic coherent effects. The lifetime of atomic coherence is longer then the atom transit time through the laser beam. Thus, the light in the wings can "probe" the induced atomic coherence and polarization of the atom coming from central parts of the laser beam. The reversed order of events, excitation of atoms first in the wings and then in the intense central parts of the laser beam will not reveal effects of the coherently prepared state due to overwhelming effects of the photons at the center of the laser beam. It is therefore a reasonable assumption that different parts of the Gaussian laser beam, after passing through the alkali vapor cell, carry different information about the atomic coherence and should yield different EIT resonances. The influence of laser beam profiles on EIT lineshapes is studied only in few papers [10–13]. The contribution of different segments of the Gaussian laser beam to the dark resonance lineshapes in a dense ^{4}He vapor was presented in Ref [13]. The results of [13] show deviation of overall resonance profile from pure Lorentzian shape attributed to observed spatial variation of lineshapes for different positions in the Gaussian beam. There are several papers showing significance of the re-excitation of atoms by separated, in space and/or time, laser beams tuned to Raman resonance of the atomic transitions. Narrowing of EIT in buffer gas cells [14, 15] and cells with antireflection coatings [16] is attributed to repeated excitation by the laser beam after the atom spends some time in 'dark', not illuminated by the laser light. The goal of this work is in part to investigate if such mechanism plays the role in observed shape of the resonance due to the light from the wings of the Gaussian laser beam.

In this work we study EIT resonances originating from different parts of the Gaussian laser beam cross-section, after the whole laser beam passes through the Rb vapor cell. Our investigation was performed on ^{87}Rb atoms at D1 line in the Hanle configuration. In the experiment, the detection of the signal from the specific parts of the Gaussian beam was accomplished by moving the aperture (placed between the Rb cell and the large area photo-detector) along the laser beam diameter. In the theoretical model, the Hanle resonance lineshapes were obtained by including the effects of the atomic polarization, the time evolution of the coherence, and the interaction of the atomic state with light in the wings of the Gaussian laser. The theoretical results distinguish the contribution to the EIT from atoms coming to the wings from central parts of the laser beam and from the outside of the beam. In line with these results, we were able to improve resonance linewidth and contrast of EIT resonances by blocking a small part of the central region of the laser beam by the small mask in front of the detector. Narrower and more contrasted resonances are important for applications of the CPT and EIT effects in atomic frequency standards [17] and magnetometry [18].

2. Experiment

The experimental setup is shown in Fig. 1. External cavity diode laser is frequency locked to $F_g=2 \rightarrow F_e=1$ transition in ^{87}Rb, where F_g and F_e correspond to angular momentum of the ground and excited state hyperfine levels, respectively. The energy level diagram, given in the insert in Fig. 1, shows magnetic sublevels of the hyperfine levels either coupled by the laser light, or populated due to spontaneous emission. Linearly polarized laser light allows for multiple Λ schemes and formation of dark states among ground Zeeman sublevels of $F_g=2$ level. The locking is performed by Doppler-free dichroic atomic vapor laser lock (DDAVLL) method [19] using auxiliary vacuum Rb cell. The variable neutral density filter is used for the laser power adjustments. The laser beam, introduced into the single mode fiber with the collimator, provides the Gaussian beam at the exit of the fiber. After passing through the Glen-Thomson polarizer the laser beam becomes linearly polarized. The laser beam is then expanded to 3 mm in diameter. The dependence of the laser intensity on the radial distance r from the beam center is Gaussian

$$I(r) = I_0 \exp\left(-2r^2/r_0^2\right),\qquad(1)$$

where I_0 is the maximal intensity and r_0 is $1/e^2$ beam radius.

The Gaussian beam passes through 5 cm long vacuum Rb cell containing natural abundance of rubidium isotopes. The cell is placed in the solenoid used for scanning the axial magnetic field between ±300 μT. The cell and the solenoid are placed inside the triple layered μ-metal cylinder to eliminate Earth's and stray magnetic fields.

The small movable aperture 0.5 mm in diameter is placed in front of the photodiode with large detection surface (area 80 mm^2). The sensitivity of the photodiode is 0.57 A/W at 780 nm and it has variable transimpedance gain with nominal value of 1 MΩ (selectable between 1 kΩ and 10 MΩ). By moving the aperture with the fine translation stage (0.25 mm shift per revolution) we are able to select specific parts of the Gaussian laser beam to reach the photodiode. The signal obtained from the photodiode while scanning the external magnetic field is recorded by the digital oscilloscope and transferred to the computer.

For some measurements we replaced the aperture with the circular mask to block the central part of the beam and detect only the outer parts of the beam.
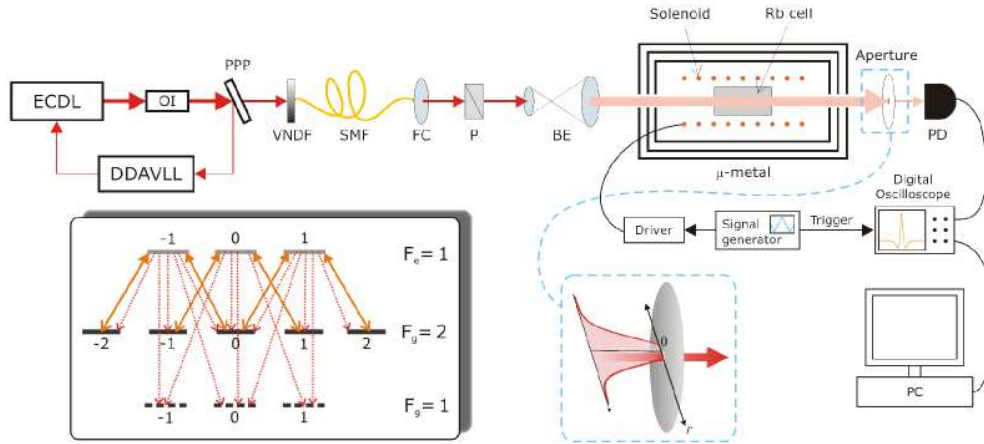

Fig. 1. Experimental setup. The aperture at translation stage allows only selected parts of the laser beam to reach detector, while the rest is blocked. ECDL – External Cavity Diode Laser, OI – Optical Isolator, DDAVLL – Doppler-free Dichroic Atomic Vapor Laser Lock, VNDF – Variable Neutral Density Filter, SMF – Single Mode Fiber, FC – Fiber Collimator, P – Polarizer, BE – Beam Expander, PD – Photodiode. Inset: The energy-level diagram for magnetic sublevels of the $F_g=2 \rightarrow F_e=1$ transition where solid lines represent linearly polarized laser light coupling Zeeman sublevels and dotted lines correspond to the de-excitation from excited levels.

3. Theoretical model

The Hanle EIT resonances were calculated for the D1 line transition $F_g=2 \rightarrow F_e=1$ of ^{87}Rb coupled by a linearly polarized laser in the Rb vacuum cell. The model is based on time dependent optical Bloch equations for the density matrix and takes into account Doppler broadening, different atomic trajectories through the laser beam, and Gaussian cylindrically symmetric radial profile of the laser electric field [12]. Rubidium atoms interact only with axially oriented homogeneous magnetic field, spatially dependent laser electric field, and cell walls. All the levels resonantly interacting with the laser light are taken into account, as well as radiative population losses to another ground state hyperfine level, $F_g=1$. After colliding with cell walls atoms reset into internal state with equally populated ground magnetic sublevels. Collisions among Rb atoms are neglected due to low Rb vapor pressure at room temperature so that the atomic trajectories through the laser beam are strait lines. For a set of atomic velocities the atomic density matrix along a given trajectory is calculated assuming constant magnetic field B during the atomic transit through the laser beam. Averaging the calculated density matrices over Maxwell-Boltzmann velocity distribution and over a collection of trajectories uniformly covering the beam cross-section, we obtain the atomic ensemble density matrix $\rho(B; r)$ across the beam for a set of radial distances r. The effects of the laser propagation along the cell and the atomic polarization of the Rb vapor are included in the following manner. Presuming that the laser intensity does not depend on the coordinate z along the laser propagation direction, we first compute the Rb vapor polarization $\mathbf{P}$ taking the constant value of the electric field $\mathbf{E}$ within the cell along the z direction. The polarization of Rb vapor of concentration n is obtained from density matrix

$$\mathbf{P}(B;r) = n\,\text{Tr}(\rho(B;r)\,e\hat{\mathbf{r}}). \tag{2}$$

Owing to the trace operation, the polarization $\mathbf{P}$ depends only on the optical coherences between the excited and the ground Zeeman sublevels. Using the computed Rb polarization, we calculate the change of the electric field due to propagation of the laser through the Rb vapor. Assuming that the change of electric field along the length L of the Rb cell is small enough, the exact relation

$$\frac{\partial \mathbf{E}(B;r,z)}{\partial z} = \frac{i\omega_0}{2\epsilon_0 c}\mathbf{P}(B;r,z), \tag{3}$$

in the first approximation takes the form

$$\mathbf{E}(B;r,z=L) = \mathbf{E}(B;r,z=0) + \frac{i\omega_0}{2\epsilon_0 c}\mathbf{P}(B;r)L, \tag{4}$$

where ε_0 is the vacuum dielectric constant and ω_0 is the laser frequency. The transmitted electric field (Eq. (4)) is used in the calculations of Hanle EIT resonances for different segments of the Gaussian beam.

4. Results and discussion

This section presents the results of the Hanle EIT resonances obtained by sampling the small parts of the laser beam after passing through the Rb gas cell. The curves in Fig. 2(a) and (b) represent the experimental and theoretical resonances recorded for different positions of the aperture along the beam diameter, with $r = 0$ mm referring to the laser beam center. The laser intensity is 0.5 mW/cm^2. There is a good agreement between the experiment and the theory. Figure 2 reveals significant differences in shapes, widths and amplitudes of the resonances at different positions within the beam. The Hanle EIT resonances from the wings of the beam show the two counter-sign peaks at certain values of the magnetic field. We suggest that the origin of such lineshape is in interaction of photons

in the wings of the laser beam with the coherently prepared atoms coming from the central part of the Gaussian beam.
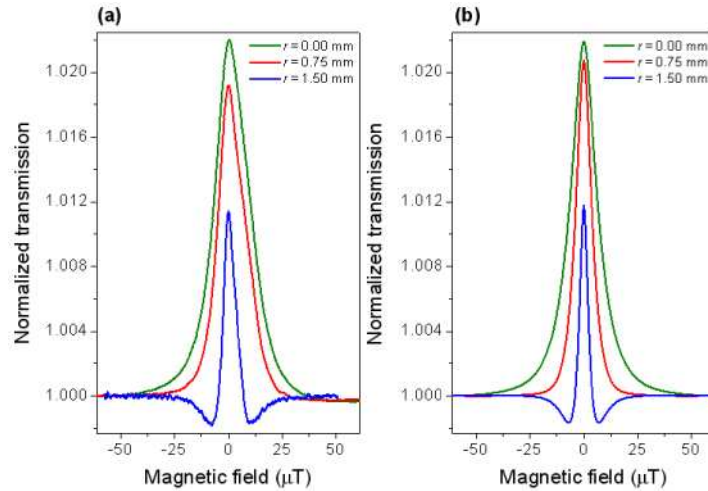

Fig. 2. Experimental (a) and theoretical (b) Hanle EIT resonances obtained from the small parts of the Gaussian beam. The green, the red and the blue curves are for $r = 0$ mm, 0.75 mm and 1.5 mm, respectively where r is the radial distance of the aperture from the beam center. The beam diameter is 3 mm and the total intensity is 0.5 mW/cm^2. Theoretical results were normalized to the experimental results such that peak values at $r = 0$ mm are equal.

During the interaction with the strong laser electric field near the center of the Gaussian beam an atom is coherently prepared into the dark state. The dark state is coherent superposition of Zeeman sublevels of $F_g=2$ ground level and is ideally non-coupled to the laser light only in the absence of external magnetic field. Zeeman sublevel populations and coherences are subjected to various relaxation processes. The transit time of the atoms through the laser beam is much shorter than the relaxation times of the ground state coherences. During the time that atom spends in the laser beam the coherences vary due to competitive effects of the laser excitation and the external magnetic field. The laser continuously forces the atomic coherence to be in-phase with the electric field. The external magnetic field causes oscillations of the coherence phase at Larmor frequency that is proportional to B. When atoms move away from the central to the outer parts of the beam (*outgoing* atoms), the oscillatory behavior prevails when the laser field is low enough. Thenceforth the phase of the atomic coherence oscillates and the atoms are cycling between dark and bright states. We name the outer section of the Gaussian beam, where this cycling occurs, *the interference region*. Aside from outgoing atoms there are also atoms coming into the interference region from the outside of the beam (*incoming* atoms). Note that the incoming atoms are not coherently prepared and do not contribute to the interference.

Consider an outgoing atom from the certain velocity class traversing the interference region along the certain trajectory. While passing through the laser beam the atom experiences nearly constant magnetic field due to its slow variation in the experiment. The phase shift of the atomic coherence at the point **r** along this trajectory depends on the value of the magnetic field B. If the coherence at **r** is in-phase with the laser electric field, the atom is in the dark state and the transparency at **r** is increased. It is clear that $B = 0$ fulfills this condition since the atom is continuously in the dark state regardless of the location in the interference region. If the magnetic field is such that the difference between the phases of the atomic coherence and the laser field equals to $\pi/2 + k\pi$ $(k \in Z)$ the atom is in the bright state, and the minima of transparency at **r** occur. We denote these minima and maxima of the transparency as interference fringes. The atoms inside the cell move with different velocities and traverse different trajectories with respect to the laser beam. The averaging over the

velocity and trajectory distributions results in the lowering of the amplitude and in washing out the higher-than-first order interference fringes in the transmission signal. These considerations are supported by the results given in Fig. 3.

Figure 3 shows Hanle EIT resonances calculated by considering outgoing, incoming and both groups of atoms. The results are given for two distances from the laser beam center, r = 1 mm (Fig. 3(a)) and r = 1.75 mm (Fig. 3(b)). It is evident that only outgoing atoms are responsible for the appearance of the two sideband transmission minima. Effect of outgoing atoms on the resonance lineshape, at certain distance r, depends on the laser intensity. Results in Fig. 3 show that for 3 mW/cm^2, the contribution of outgoing atoms to Hanle EIT resonances is negligible at the distance r = 1 mm, while it is very strong at r = 1.75 mm.

The physical mechanism used in the above explanation of our results is the same as in Raman-Ramsey interference. The resulting Hanle lineshapes are similar to those obtained due to Ramsey interference in separated pump and probe laser fields in vacuum gas cells [20]. In our case, the extended low intensity wings of the Gaussian laser beam play the role of the probe beam.
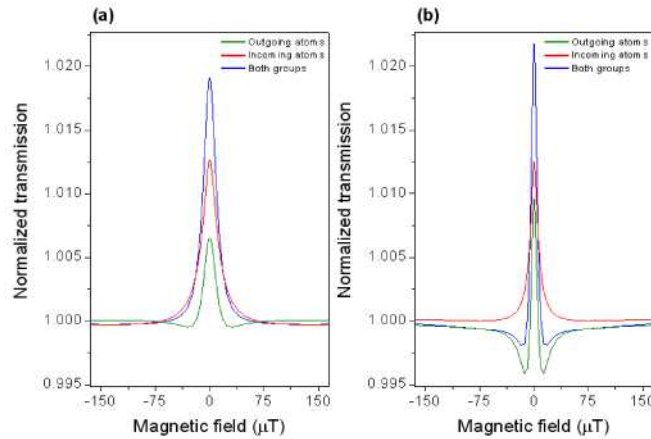

Fig. 3. Calculated contribution of outgoing (green), incoming (red) and both outgoing and incoming (blue) atoms to the Hanle EIT resonances for two distances from the laser beam center: r = 1.00 mm (a) and r = 1.75 mm (b). The total laser intensity is 3 mW/cm^2.

Figure 4 shows experimental (a) and theoretical (b) behavior of the Hanle EIT linewidths as a function of the aperture radial position. There are two reasons for narrowing of the Hanle EIT resonances in the wings of the Gaussian laser beam profile. The first is the lower power broadening in the outer parts of the laser beam. Another reason is the Ramsey-like narrowing caused by the aforementioned physical processes. The line narrowing at larger radial distances becomes more prominent as the total laser intensity increases. The dashed bars in (a) denote the linewidths of the Hanle EIT resonances for the three laser beam intensities when the whole laser beam is detected. At this point we find suitable to compare with results of Ref [13]. Lineshape Rabi power broadening corresponding to local intensities within the Gaussian beam, was also observed in [13] but without altering local resonance Lorentzian shape due to interference effects. We consider that one possible reason for the absence of the interference effects in such experiment is due to short mean free path of ^{4}He atoms. Namely, at the pressure of 1.5 Torr the mean free path of ^{4}He atoms is of the order 0.1 mm, so that ^{4}He atoms are effectively localized and do not freely traverse the 6 mm diameter laser beam. Therefore, the interference effects could not occur in the experiment performed in [13] due to frequent atom-atom collisions.

The outer, less intense, parts of the Gaussian beam, contribute with quite narrower lines to the overall Hanle EIT resonance. Thus, we studied Hanle EIT resonances after blocking the central part of the Gaussian beam in front of the detector. Figure 5(a) presents the Hanle EIT curves obtained when the mask of 2.2 mm in diameter blocks the central part of the Gaussian

beam (red curve). The resonance obtained without the mask is shown by the green curve. In Fig. 5(b) and (c) the dependence of linewidth and contrast of the EIT on the beam intensity is shown, with and without the mask. It is obvious that if one blocks the central part of the Gaussian laser beam, the Hanle EIT resonances will be significantly narrower for the range of the laser intensities used in the experiment. Apparently, this masking effect is more prominent at higher laser intensities. In cases of higher laser intensities masking provides also the resonances with higher contrast. Narrower and more pronounced resonances obtained in the proposed manner could be very useful for various applications of EIT.
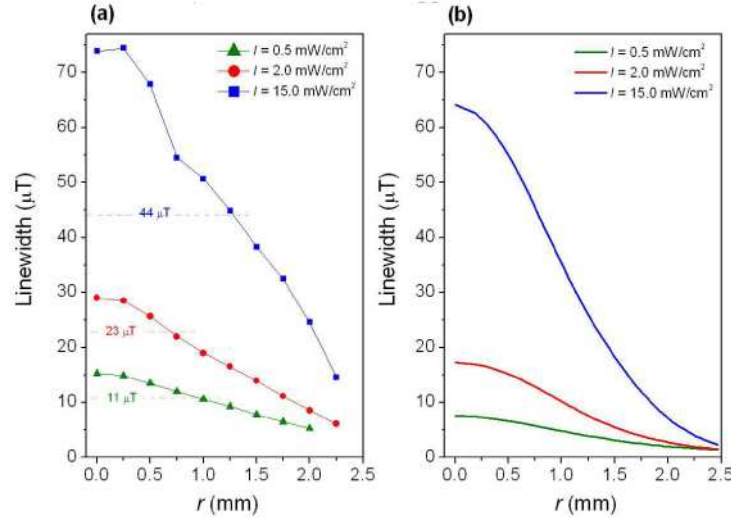

Fig. 4. Experimental (a) and theoretical (b) Hanle EIT linewidths for the different positions *r* of the aperture along the laser beam diameter. The blue, the red, and the green curves are for the intensities *I* = 15 mW/cm^2, 2 mW/cm^2, and 0.5 mW/cm^2, respectively. The dashed bars in (a) represent the Hanle EIT linewidths obtained by detecting the whole laser beam.
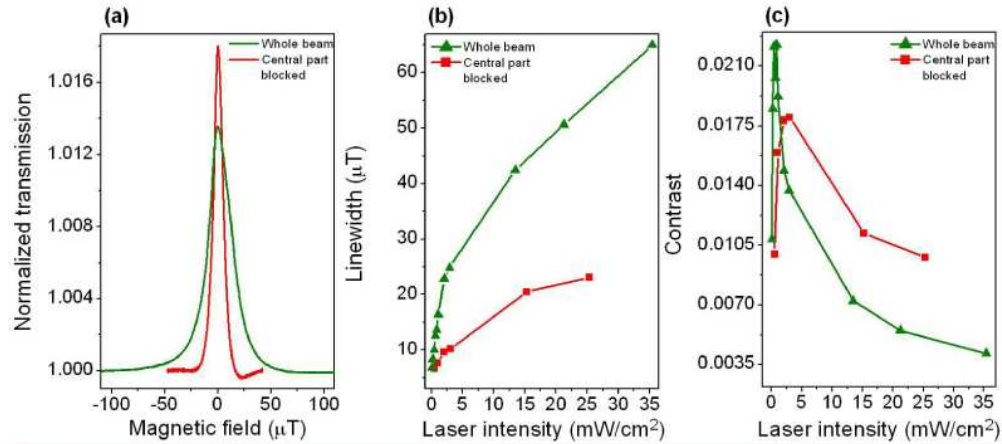

Fig. 5. (a) The experimental Hanle EIT resonances obtained when the whole beam is detected (green curve) and when the central part of the beam is blocked in front of the detector (red curve). In (b) and (c) linewidth and contrast of the EIT versus laser intensity are given for the whole beam (green) and for the beam with blocked central part (red). The central part was blocked by circular mask of diameter *d* = 2.2 mm. The laser intensity is 3 mW/cm^2.

5. Conclusion

In this work we have presented results of the Hanle EIT obtained from selected parts of the cross-section of the Gaussian laser beam, after the entire laser beam passes the Rb vacuum cell. The lineshapes, widths and contrasts of the EIT depend on the radial position of the sampled area of the laser beam. The resonances originating from the central part are different then those originated from the wings of the Gaussian. In the latter case the resonances are much narrower with two counter-sign sideband peaks. Our theoretical model reproduces the experimental EIT and explains the obtained EIT lineshapes by the interference between the atomic coherence carried by the coherently prepared atoms and the laser light in the wings of the Gaussian. The model shows that narrowing and interference features in the lineshapes are due to atoms coming from the central parts of the laser beam. These features are partially masked due to simultaneous contribution from atoms coming from the outside of the laser beam. Considerable improvement of the EIT linewidths and even contrasts is obtained by blocking the central part of the Gaussian beam in front of the photodiode and detecting only light from the wings of the laser beam. Narrowing of EIT in vacuum gas cells are of interests in EIT applications for atomic frequency standards and magnetometers.

Acknowledgements